Available online at www.sciencedirect.com

ScienceDirect

IFAC PapersOnline CONFERENCE PAPER ARCHIVE

IFAC PapersOnLine 56-2 (2023) 10721–10726

Swarm Model for Path Tracking with Reference Motion Profile: a Diffeomorphism-based Approach

A. Bono * **B. Chen** ** **L. D'Alfonso** * **G. Fedele** *

* *Dept. of Computer Engineering, Modeling, Electronics and Systems, Università della Calabria, Via Pietro Bucci, Cubo 42-C, Rende (CS), 87036, Italy (e-mail: {antonio.bono,luigi.dalfonso,giuseppe.fedele}@unical.it).*

** *Dept. of Electronic and Electrical Engineering, University College London, London WC1E 6BT, U.K. (e-mail:boli.chen@ucl.ac.uk).*

Abstract: This paper presents a novel strategy to control a multi-agent system along a given reference path while ensuring compliance with a given time profile for the movements along the route in question. The proposed protocol is based on a three-step methodology. In a first step, each agent state is augmented with an artificial variable that defines the movement of the agents along the given path. The extended agent state is then mapped into a virtual frame that takes into account the displacement of its position with respect to the reference path and the control over the additional artificial variable. Finally, in a third step, the control law designed in the artificial frame is translated into an action in the real frame using the theory of diffeomorphisms. The proposed control strategy ensures finite-time convergence of the entire multi-agent system on the reference path, while achieving error bounding for each agent evolution with respect to a given reference motion profile. Numerical simulations are performed to illustrate the described results.

Keywords: Multi-agent system, Finite-time control, Distributed path tracking, Swarm of agents, Diffeomorphism-based control.

1. INTRODUCTION

A multi-agent system consists of several interacting intelligent agents that, by exploiting their communication, can solve problems that would be difficult or even impossible for a single, individual agent or a monolithic system to solve (see Hu et al. (2021a,b)). A growing number of applications benefit from the coordination and cooperation of multiple autonomous agents to achieve a group goal. The main ideas behind agent flock studies were first proposed by Reynolds (1987), where the flight behaviour of a flock of birds was modelled as a group of agents, where each bird follows a set of simple rules and interacts with others in its neighborhood. Other examples of biological swarming can be found in fish schools, insect swarms, bacterial swarms and quadruped herds, as described in Warburton and Lazarus (1991). The spontaneous emergence of collective behaviours in animal groups and in biological and social networks has inspired several engineering applications (see Mwaffo et al. (2021)), in which groups of agents coordinate themselves by exploiting local interactions between individuals to achieve multiple benefits for the whole team: more efficient foraging or more effective defence against predators (see Chipade and Panagou (2021); Gazi and Passino (2011); Dunbabin and Marques (2012); Egerstedt and Hu (2001)).

In the multitude of research topics of interest related to swarms, the coordinated movement of multiple vehicles has attracted the control community in recent decades due to its wide range of applications (see Schranz et al. (2020)). This type of synchronised movement in a multi-agent system is usually referred to as formation control and its solutions require an orderly arrangement of vehicles during movement (Dong et al. (2016); Fedele and D'Alfonso (2018)). A special case of formation control is the control of vehicle platoons, where several interconnected vehicles (agents) move in a string-like formation, maintaining a close distance between vehicles to reduce fuel consumption (Liang et al. (2015)). This type of formation control problem has been approached in several ways: Consensus-based control has been applied by Zheng et al. (2015), D'Alfonso et al. (2018) uses a model predictive control strategy, while Gao et al. (2018) and Li et al. (2017) use sliding mode control and robust control, respectively.

Although the literature has dealt extensively with platoon control, the proposed solutions are generally based on control schemes in which the movement to be imposed on the agents is considered as a reference time trajectory to be followed (Xu et al. (2019)). In contrast, the idea in the present work is to use a suitable parametrisation of the path (i.e. road) on which the multi-agent system is to travel, separating the problem of reaching such a path from the problem of moving along it. In other words, an appropriate diffeomorphism is used to translate the movement of each agent into a part related to reaching the desired path and a part related to the desired movement profile

10.1016/j.ifacol.2023.10.730

on that path. In this way, imposing different movement profiles on the same reference path becomes a very trivial task.

The entire control protocol will conform to the *map-design-map back* scheme. First, the multi-agent system will be enriched with a set of artificial variables to augment each agent dimension. This augmented swarm is then mapped into a virtual reference frame, exploiting the parameterisation of the road on which the agents must be driven, which takes into account position errors with respect to the reference path and movement errors with respect to a given target movement profile. In this novel reference frame, a virtual control law is designed, which is then fed back to the real reference frame to control the real multi-agent system. As mentioned before, the proposed control strategy ensures finite-time convergence of the swarm to the target path while achieving a bounded motion error with respect to the desired movement profile on the target path.

The paper is organized as follows. Section 2 describes the problem to address. Section 3 defines the proposed strategy to solve the problem in terms of the used reference frames mapping. The multi-agent system model and its main properties are described in Section 4. Section 5 provides numerical simulations to highlight the obtained theoretical results. Last section is devoted to conclusions.

Notation

The following conventions and notations are used throughout the paper:

- $\mathbb{R}_{\geq 0}\,(\mathbb{R}_{>0})$ is the set of non-negative (positive) reals;
- $\mathbb{N}^{+}$ is the set of integer numbers greater than 0;
- 0_k is the $k \in \mathbb{N}^{+}$ dimensional zero vector;
- $\mathbb{I}_k$ is the identity matrix of order $k \in \mathbb{N}^{+}$;
- given a vector $v \in \mathbb{R}^n$, its cartesian coordinates are denoted as $v_1,\ v_2, \ldots, v_n$;
- given $x \in \mathbb{R}$, the signum function is defined as
$$\text{sign}(x) = \frac{|x|}{x} = \begin{cases} -1, & \text{if } x < 0, \\ 0, & \text{if } x = 0, \\ 1, & \text{if } x > 0; \end{cases}$$
- $\mathcal{G} = \{V, E\}$ is an undirected graph consisting of a nonempty finite set of vertices $V = \{v_i,\ i = 1, ..., n\}$ and of a set of unordered pairs of vertices $E \subseteq \{(v_i, v_j)\ :\ v_i, v_j \in V,\ v_i \neq v_j\}$ representing the edges of the graph. When an edge exists between vertices v_i and v_j, they are called adjacent. The set of neighbours of node v_i is denoted by $\mathcal{N}_i = \{v_j \in V \backslash \{v_i\}\ :\ (v_i, v_j) \in E\}$.

2. PROBLEM STATEMENT

This section defines the problem of interest and the characteristics that its solution must fulfil.

Consider a swarm of $\nu \in \mathbb{N}^{+}$ agents modeled as kinematic points moving in $\mathbb{R}^n,\ n \in \mathbb{N}^{+}$:
$$\dot{z}_i(t) = u_i(t),\ i = 1, \ldots, \nu \tag{1}$$
and assume that the agents can interact with each other as defined by the communication topology $\mathcal{G}$. In particular, the standard approach is to model the interaction between agents by an undirected graph $\mathcal{G}$ consisting of agents as nodes of the graph and interactions due to perception and communication as edges of the graph.

Consider now a continuous and differentiable curve in $\mathbb{R}^n$, $\gamma \in \mathcal{C}^1$, with $\gamma : \mathbb{R} \to \mathbb{R}^n$, representing a given path or a shape defined in cartesian coordinates as
$$\gamma(\omega) = [\gamma_1(\omega),\ \ldots,\ \gamma_n(\omega)]^T \tag{2}$$
and related to the variable $\omega \in \mathbb{R}$ for its continuous parametrization. For a path moving exactly on γ, a motion profile can be chosen by describing the time evolution, namely $\omega(t)$, and looking at the resulting value of the curve, i.e. $\gamma(\omega(t))$. The problem to be solved can now be defined as follows.

Path tracking on a curve problem (PTCP)

Given the set of agents defined in (1), assume a coherent communication topology and a curve $\gamma(\omega)$ as defined in (2) with a target movement profile for the path on the curve, i.e. $\bar{\omega}(t)$, find a control protocol $u_i(t),\ i = 1, \ldots, \nu$, to ensure that:

- C1 each agent reaches and remains on $\gamma(\omega)$ without ever leaving its contour, i.e. there exists a time τ such that the multi-agent system defined by $z_i(t),\ i = 1, \ldots, \nu$ moves on $\gamma(\omega)$ for each $t \geq \tau$;
- C2 the movements of the agents on γ are asymptotically related to the movement profile of the reference target $\bar{\omega}(t)$, so that
  - a velocity consensus is achieved:
$$\lim_{t\to\infty} \left(\dot{z}_i(t) - \frac{\partial \gamma(\omega)}{\partial \omega}\bigg|_{\bar{\omega}(t)} \dot{\bar{\omega}}(t) \right) = 0_n,\ \forall i; \tag{3}$$
  - the positions of the agents are in a bounded region with respect to the reference positions defined by $\bar{\omega}(t)$:
$$\exists \Delta_z > 0\ s.t.\ \lim_{t\to\infty} \|z_i(t) - \gamma(\bar{\omega}(t))\| \leq \Delta_z, \forall i. \tag{4}$$

In other words, a control law must be designed that steers the agents on the curve $\gamma(\cdot)$ in such a way that they move exactly on this curve, respecting a motion profile defined by $\bar{\omega}(t)$, with a bounded error with respect to the reference trajectory $\gamma(\bar{\omega}(t))$.

3. REFERENCE FRAMES MAPPING

To solve the PTCP, the main idea is to use a mapping between the reference frame in which the multi-agent system is defined and a new frame in which the errors between the agents' states and the target curve are taken into account together with a tracking error with respect to the movement profile $\bar{\omega}(t)$. Going deeper, it is assumed that each agent state is artificially augmented by another variable, $\omega_i(t) \in \mathbb{R}$, representing its current state on the curve γ, i.e. the following new set of agents is defined
$$\zeta_i(t) = \left[z_i^T(t),\ \omega_i(t)\right]^T,\ i = 1, \ldots, \nu$$
assuming that the initial conditions $\omega_i(0) \neq \omega_j(0)$ are chosen for each pair (i, j) of agents, and with the corresponding augmented model
$$\dot{\zeta}_i(t) = \mathcal{U}_i(t) = \left[u_i^T(t),\ u_{\omega,i}(t)\right]^T,\ i = 1, \ldots, \nu \tag{5}$$

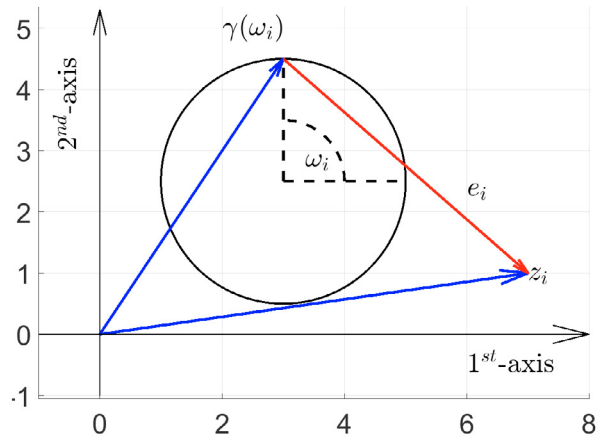

Fig. 1. Example of mapping from z_i to e_i considering the case of 2-dimensional agents with $\omega_i = \frac{\pi}{2}$ and $\gamma(\omega)$ as a circle centered in $[3, 2.5]^T$ with radius of 2 meters.

where the artificial control action $u_{\omega,i}(t) \in \mathbb{R}$ was also used to augment the control signal.

At this point by defining the error signal as

$$e_i(t) \triangleq z_i(t) - \gamma(\omega_i(t)),$$

see Fig. 1, a diffeomorphism associated with a virtual mapping from $\zeta_i(t)$ to a virtual agent

$$\mathcal{E}_i = \left[e_i(t)^T,\ \omega_i(t)\right]^T \tag{6}$$

can be considered and used to translate the evolution of the agents in the real reference frame into an evolution where the discrepancies in terms of $\gamma(\cdot)$ are taken into account together with the movement profile of each agent on the curve. In particular, in the new frame where agents move $\mathcal{E}_i, i = 1, \dots, \nu$, if the first n coordinates of each agent go to zero and remain stable, and if the last coordinate follows the reference $\bar{\omega}(t)$ with bounded error and a velocity consensus, i.e. $|\omega_i(t) - \bar{\omega}(t)|$ is bounded and $\dot{\omega}_i = \dot{\bar{\omega}}(t)$, then the PTCP would be solved in the real reference frame.

For the sake of completeness, we recall below a useful property of diffeomorphism that applies to the dynamic evolution of a mathematical model.

Lemma 1. Consider a system $\dot{x}(t) = f(x(t))$ and the diffeomorphism $x = h(y)$. Then the system evolution in the new variable results in

$$\dot{y}(t) = \left(\mathcal{J}(y(t))\right)^{-1} f(x(t))$$

where $\mathcal{J}(y(t)) \triangleq \left.\frac{\partial}{\partial y} h\right|_{y(t)}$ is the jacobian of the diffeomorphism computed in $y(t)$ (see Banyaga (2013)).

Therefore, Lemma 1 can be used to map the solution obtained in the auxiliary reference frame to the real one. The proposed overall solution is then composed of three main steps:

(1) Convert $\zeta_i(t),\ i = 1, \dots, \nu$ to related virtual agents $\mathcal{E}_i(t)$ as defined by the diffeomorphism in (6).
(2) Assuming a model $\dot{\mathcal{E}}_i(t) = \mathcal{U}_{\mathcal{E},i}(t)$, design the control law $\mathcal{U}_{\mathcal{E},i},\ i = 1, \dots, \nu$ to solve the modified version of the PTCP in the artificial reference frame as described earlier.
(3) Convert the artificial control law back to the real one using Lemma 1 as

$$\mathcal{U}_i(t) = \left[\mathcal{J}(t)\right]^{-1} \mathcal{U}_{\mathcal{E},i}(t)$$

with the Jacobian of the diffeomorphism obtained as

$$\mathcal{J}(t) = \left[\begin{array}{c|c} \mathbb{I}_n & -\dfrac{\partial}{\partial \omega}\gamma(\omega) \\ \hline 0_n^T & 1 \end{array}\right]\Bigg|_{\zeta_i(t)}.$$

4. MULTI-AGENT SYSTEM PROPERTIES

In this section, the defined problem is solved in the auxiliary frame so that to obtain a control signal that is converted into the real frame, as defined in the previous section. In particular, the following artificial control law is proposed

$$\mathcal{U}_{\mathcal{E},i}(t) = \begin{bmatrix} u_{e,i}(t) \\ u_{\omega,i}(t) \end{bmatrix} = \begin{bmatrix} -e_i(t) - \sigma_i(t) \\ -(\omega_i(t) - \bar{\omega}(t)) + q_i(t) + \dot{\bar{\omega}}(t) \end{bmatrix} \tag{7}$$

where, given $\mu \in (0, 1)$, $\beta \in \mathbb{R}_{>0}$ and denoted as $e_{i,k}$, $k = 1, \dots, n$ the k-th coordinate of e_i,

- $u_{e,i} \in \mathbb{R}^n$ accounts for the evolution of $e_i(t)$ and $\sigma_i(t) = [\sigma_{i,1}(t), \dots, \sigma_{i,n}(t)]^T$ with
$$\sigma_{i,k}(t) = sign(e_{i,k}(t))|e_{i,k}(t)|^{\mu};$$
- the signal $q_i(t) \in \mathbb{R}$ models the interaction between the artificial signals ω_i, $i = 1, \dots, \nu$ as
$$q_i(t) = \beta \sum_{j \in \mathcal{N}_i} g(|\omega_i(t) - \omega_j(t)|)(\omega_i(t) - \omega_j(t)).$$
The function $g(\cdot) : \mathbb{R}_{\geq 0} \to \mathbb{R}_{\geq 0}$ represents the interaction force between two agents along the artificial axis on which $\omega_i, i = 1, \dots, \nu$ evolves and is assumed to satisfy the following properties

$$\exists J(\|p\|) : \mathbb{R} \to \mathbb{R}\ s.t.\ \frac{d}{dp} J(|p|) = -g(|p|)p \tag{8}$$

$$\exists \delta \in \mathbb{R}_{\geq 0} : \begin{cases} g(|p|)|p| \leq \delta \\ \vee \\ g(|p|)|p| \leq \delta/|p|. \end{cases} \tag{9}$$

As for (9), it is fulfilled if $g(\cdot)$ is compliant with one of the defined conditions, and depending on which one is satisfied, the defined interaction function $g(\cdot)$ will provide for bounded or unbounded repulsion effect between ω_i and ω_j (see Fedele et al. (2022)). Both cases are analysed below.

As a first result, the asymptotic behaviour of the artificial signals ω_i shall be investigated.

Theorem 2. The artificial signals $\omega_i(t),\ i = 1, \dots, \nu$, whose evolution is determined by (5) and (7), asymptotically reach a configuration where their centroid goes to the target motion profile $\bar{\omega}$, i.e.

$$\lim_{t \to \infty} \left(\frac{1}{\nu} \sum_{i=1}^{\nu} \omega_i(t) - \bar{\omega}(t) \right) = 0.$$

Proof. Let $V = \frac{1}{2}\left[\frac{1}{\nu}\sum_{i=1}^{\nu}(\omega_i(t) - \bar{\omega}(t))\right]^2$ be a candidate Lyapunov function. Its derivative results in

$$\dot{V} = \frac{1}{\nu^2}\left[\sum_{i=1}^{\nu}(\omega_i-\bar{\omega})\right]\sum_{i=1}^{\nu}(\dot{\omega}_i-\dot{\bar{\omega}}) = -\frac{1}{\nu^2}\left[\sum_{i=1}^{\nu}(\omega_i-\bar{\omega})\right]^2$$

where the time dependency has been omitted for the sake of clarity. □

Let us now analyse the evolution of the discrepancy signals $e_i(t),\ i=1,\dots,\nu$. In particular, it is shown that these signals approach zero at steady-state and further properties are given for the transient time until the steady-state value is reached.

Theorem 3. The signals $e_i(t),\ i=1,\dots\nu$, evolving according to (5) and (7), reach 0_n in finite time:

$$\exists \tau > 0 \ s.t.\ e_i(t) = 0_n,\ \forall t \geq \tau,\ \forall i.$$

Proof. The evolution of $e_i(t)$ can be viewed as a set of n independent equations, one for each of its components. To prove the convergence to zero of each component $e_{i,k}, k = 1,\dots,n,\ i=1,\dots,\nu$, consider the candidate Lyapunov function $V_{i,k}(t) = \frac{1}{2}e_{i,k}^2$, whose derivative is

$$\begin{aligned}\dot{V}_{i,k} &= e_{i,k}\dot{e}_{i,k} = e_{i,k}\left(-e_{i,k} - sign(e_{i,k})|e_{i,k}|^{\mu}\right) = \\ &= -e_{i,k}^2 - |e_{i,k}|^{\mu+1} \leq -|e_{i,k}|^{\mu+1} = -\frac{2^{\frac{\mu+1}{2}}|e_{i,k}|^{\mu+1}}{2^{\frac{\mu+1}{2}}} = \\ &= -2^{\frac{\mu+1}{2}}\left(\frac{e_{i,k}^2}{2}\right)^{\frac{\mu+1}{2}} = -2^{\frac{\mu+1}{2}}\left(V_{i,k}\right)^{\frac{\mu+1}{2}}\end{aligned}$$

that, as described by Fedele et al. (2018), ensures finite time convergence to zero after $\tau_i = \max_{k=1,\dots,n}\frac{V_{i,k}^{1-\eta}(0)}{2^{\eta}(1-\eta)}$ with $\eta = \frac{\mu+1}{2}$. Defining now $\tau = \max_{i=1,\dots,\nu}\tau_i$ the proof follows. □

The above result explains the compliance with condition C1 of PTCP when the control law is mapped back to the original reference frame, since the error between $z_i(t)$ and the moving point $\gamma(\omega_i(t))$ reaches and remains zero. The next results give information about the stationary positions that the agents reach around $\gamma(\bar{\omega}(t))$.

Theorem 4. The signals $\omega_i(t),\ i=1,\dots,\nu$ ruled by (7) asymptotically reach a bounded region around $\bar{\omega}(t)$, i.e.

$$\exists \Delta_\omega \in \mathbb{R}_{>0}\ s.t.\ \lim_{t\to\infty}|\omega_i(t)-\bar{\omega}(t)| \leq \Delta_\omega,\ i=1,\dots,\nu.$$

Proof. Let $w_i(t) \triangleq \omega_i(t) - \bar{\omega}(t)$ define the error between ω_i and the reference, then the error evolution yields

$$\dot{w}_i = -w_i + \beta\sum_{j\in\mathcal{N}_i} g(|w_i-w_j|)(w_i-w_j). \qquad (10)$$

The proof now changes depending on which condition in (9) is satisfied; in other words, depending on the boundedness of $g(\cdot)$, a different value for Δ_ω can be found.

Bounded interaction: $g(|p|)|p| \leq \delta$

Consider the candidate Lyapunov function $V(t) = \frac{1}{2}w_i^2(t)$ with $\dot{V}(t) = -w_i^2(t) + \beta\sum_{j\in\mathcal{N}_i} w_i g_{ij}(w_i-w_j)$ where the notation $g_{ij} = g(|w_i(t)-w_j(t)|)$ was used for clarity. It follows that

$$\begin{aligned}\dot{V}(t) &\leq -w_i^2(t) + \beta\sum_{j\in\mathcal{N}_i}|w_i(t)|g_{ij}|w_i(t)-w_j(t)| \leq \\ &\leq -w_i^2(t) + \beta|w_i(t)|(\nu-1)\delta\end{aligned}$$

that is $\dot{V}(t) \leq 0$ until $|w_i(t)| \geq \beta(\nu-1)\delta$ which means that $|\omega_i(t)-\bar{\omega}(t)|$ takes a value bounded by $\Delta_\omega = \beta(\nu-1)\delta$.

Unbounded interaction: $g(|p|)|p| \leq \delta/|p|$

Let $V(t) = \frac{1}{2}\sum_{i=1}^{\nu} w_i^2(t)$ be a candidate Lyapunov function. Considering the set E of all the edges in the topology graph of the multi-agent system, the derivative of $V(t)$ can be written as follows:

$$\begin{aligned}\dot{V} &= \sum_{i=1}^{\nu} w_i\dot{w}_i = \sum_{i=1}^{\nu} w_i\left(-w_i + \beta\sum_{j\in\mathcal{N}_i} g_{ij}(w_i-w_j)\right) = \\ &= -\sum_{i=1}^{\nu} w_i^2 + \beta\sum_{(i,j)\in E} g_{ij}(w_i-w_j)^2\end{aligned}$$

where $\sum_{i=1}^{\nu}\sum_{j\in\mathcal{N}_i} g_{ij}w_i(w_i-w_j) = \sum_{(i,j)\in E} g_{ij}(w_i-w_j)^2$ has been used (see Mesbahi and Egerstedt (2010)).

Now considering the property $g(|p|)|p| \leq \delta/|p|$, it follows that $\dot{V}(t) \leq -\sum_{i=1}^{\nu} w_i^2(t) + \beta\frac{\nu(\nu-1)}{2}\delta$ is certainly less than zero if at least one agent $w_i^2(t) \geq \beta\frac{\nu(\nu-1)}{2}\delta$. Therefore, $\Delta_\omega = \sqrt{\beta\frac{\nu(\nu-1)}{2}\delta}$ can be chosen. □

The result of the Theorem 4 ensures that the agents in the real reference frame reach a bounded region around the target $\gamma(\bar{\omega}(t))$, so that the second part of condition C2 in the definition of PTCP is satisfied. In particular, $\Delta_z = \max_t \max_{\omega\in[\bar{\omega}(t)-\Delta_\omega,\bar{\omega}(t)+\Delta_\omega]}\|\gamma(\omega)-\gamma(\bar{\omega}(t))\|$.

Theorem 5. The artificial signals $\omega_i(t),\ i=1,\dots,\nu$ driven by the control law in (7) asymptotically reach a velocity consensus at $\dot{\bar{\omega}}(t)$, i.e. $\lim_{t\to\infty}(\dot{\omega}_i(t)-\dot{\bar{\omega}}(t)) = 0,\ i=1,\dots,\nu$.

Proof. Consider the model in (10) and the function

$$\Xi(t) = \sum_{i=1}^{\nu} w_i^2 + \beta\sum_{i=1}^{\nu}\sum_{j\in\mathcal{N}_i} J(|w_i-w_j|)$$

then

$$\begin{aligned}\dot{\Xi} &= \sum_{i=1}^{\nu} 2w_i\dot{w}_i + \beta\sum_{i=1}^{\nu}\sum_{j\in\mathcal{N}_i}\left(\frac{\partial J}{\partial w_i}\dot{w}_i + \frac{\partial J}{\partial w_j}\dot{w}_j\right) = \\ &-2\sum_{i=1}^{\nu}\dot{w}_i^2 + 2\beta\sum_{i=1}^{\nu}\sum_{j\in\mathcal{N}_i} g_{ij}(w_i-w_j)\dot{w}_i + \\ &+\beta\sum_{i=1}^{\nu}\sum_{j\in\mathcal{N}_i}\left(\frac{\partial J}{\partial w_i}\dot{w}_i + \frac{\partial J}{\partial w_j}\dot{w}_j\right)\end{aligned}$$

where $2w_i = 2\left(-\dot{w}_i + \beta\sum_{j\in\mathcal{N}_i} g_{ij}(w_i-w_j)\right)$ has been used. By exploiting now (8), it follows that

$$\dot{\Xi} = -2\sum_{i=1}^{\nu} \dot{w}_i^2 + 2\beta \sum_{i=1}^{\nu}\sum_{j\in\mathcal{N}_i} g_{ij}(w_i - w_j)\dot{w}_i + \\ -\beta\sum_{i=1}^{\nu}\sum_{j\in\mathcal{N}_i} g_{ij}(w_i - w_j)\dot{w}_i - \beta\sum_{i=1}^{\nu}\sum_{j\in\mathcal{N}_i} g_{ij}(w_i - w_j)\dot{w}_j$$

where the sum of the last terms of the r.h.s. is zero due to the reciprocity of the neighbourhood of each agent and then $\dot{\Xi} = -2\sum_{i=1}^{\nu} \dot{w}_i^2$. Since the evolution of w_i is bounded according to the Theorems 3 and 4, LaSalle's Invariance Principle (Khalil (2002)) ensures that the agents asymptotically converge to the largest invariant set in $\{w \in \mathbb{R} \mid \dot{\Xi} = 0\}$, i.e., all signals ω_i converge to a fixed configuration with respect to $\bar{\omega}(t)$ and a velocity consensus at $\dot{\bar{\omega}}(t)$ is achieved. □

The last result, translated into the real frame of reference, ensures the fulfilment of the first part of condition C2 in the definition of PTCP. In summary, the model defined by (5) using the diffeomorphism in (6) and the control law proposed in (7) ensures that PTCP is solved.

5. NUMERICAL SIMULATIONS

In order to highlight the main features of the proposed solution, two numerical simulations were carried out. In both simulations, a set of $\nu = 5$ agents was used, with initial conditions randomly chosen in a square with a side of 5 meters and centred at $[-3, -3]^T$. As for the artificial signals ω_i, $i = 1, \dots, \nu$, their initial values were chosen randomly in a line of length 20 and centred at zero.

Example 1. In the first simulation, the five agents were controlled to track the path

$$\gamma(\omega(t)) = \left[\omega(t),\ 10(1 - Ae^{-\xi\psi\omega(t)}\sin(2\psi A^{-1}\omega(t) + \phi))\right]^T$$

with $A = 1.005$, $\psi = 1.4706$, $\xi = 0.1$ and a reference motion profile $\bar{\omega}(t) = t$. The parameters $\mu = 0.5$, $\beta = 10$ were fixed; the connectivity between agents was encoded by the following Laplacian matrix

$$\mathcal{L} = \begin{bmatrix} 1 & 0 & 0 & 0 & -1 \\ 0 & 2 & -1 & -1 & 0 \\ 0 & -1 & 3 & -1 & -1 \\ 0 & -1 & -1 & 3 & -1 \\ -1 & 0 & -1 & -1 & 3 \end{bmatrix}$$

and an unbounded interaction function $g(|p|) = 1/p^2$, related to $J(p) = -\log(|p|)$ and $\delta = 1$, was used. The overall results are shown in Figs. 2 and 3. The former shows the evolution of the multi-agent system in some time snapshots while the latter shows the finite time convergence of $e_i(t)$, $i = 1, \dots, \nu$ and the boundedness of $|\omega_i(t) - \bar{\omega}(t)|$, $i = 1, \dots, \nu$.

Example 2. The five agents were driven on the circular shape $\gamma(\omega(t)) = [3\cos(\omega(t)),\ 3\sin(\omega(t))]^T$ with a reference motion profile $\bar{\omega}(t) = 5\sin(0.5t)$. The parameters $\mu = 0.5$, $\beta = 100$ were set and full connectivity between the agents was assumed. The bounded interaction function $g(|p|) = (|p|^2 + \varepsilon)^{-1}$ with $\varepsilon = 0.01$, related to $J(p) = -(1/2)\log(p^2 + \varepsilon)$ and $\delta = (1/2)\varepsilon^{-\frac{1}{2}}$ (see Fedele and D'Alfonso (2019)), was used. The results obtained are shown in Fig. 4 with 4 time snapshots highlighted. In particular, the first snapshot represents the initial conditions of the agents, while the others highlight the evolution of the multi-agent system and the direction of motion of each agent on the reference curve. At $t = 10s$ and $t = 22s$ the agents move counterclockwise while at $t = 45s$ they move clockwise, as prescribed by the chosen $\bar{\omega}(t)$.

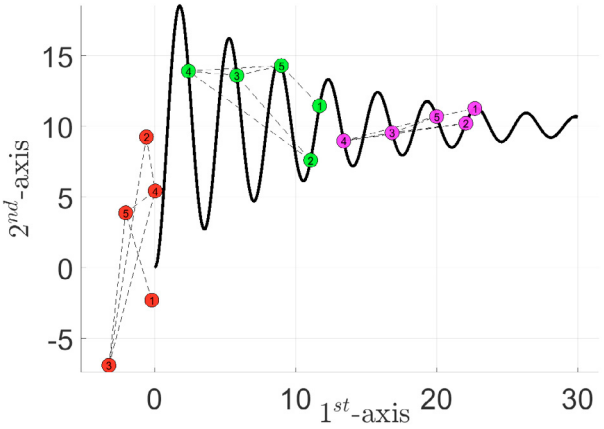

Fig. 2. Example 1: Reference shape $\gamma(\omega)$, in black, and three snapshots of agents' configuration at $t = 0s$ (red circles), $t = 8s$ (green circles) and $t = 19s$ (magenta circles). The agents have been labeled and the dashed lines represent the connectivity as ruled by $\mathcal{L}$.

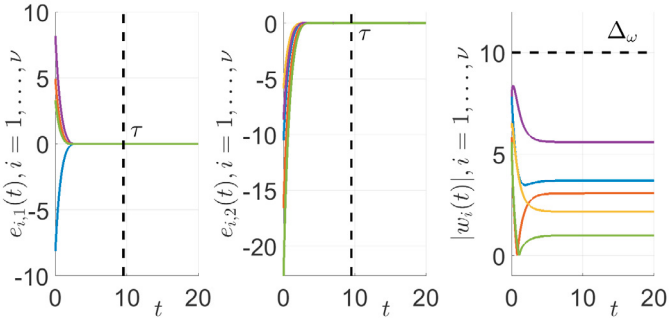

Fig. 3. Example 1: Error signals evolution $e_{i,1}(t)$ (on the left), $e_{i,2}(t)$ (on the center) and $|w_i(t)|$ (solid lines on the right), $i = 1, \dots, \nu$. The values of τ and Δ_ω, computed as defined in Theorems 3 and 4 respectively, are shown (as black dashed lines) to highlight the convergence and boundedness properties.

6. CONCLUSIONS

This paper is concerned with the design of a control protocol for a multi-agent system that enables a platoon formation along a desired path and with a given movement profile. A three-step strategy based on the theory of diffeomorphisms has been described. The main steps are to augment each agent state with an artificial variable that defines the movement of the agents on the prescribed path; to map this novel state into a virtual framework that accounts for the shift in the pose of the agents with respect to the reference route and the control over the additional artificial variable; to map the designed virtual control law back to a real one. The proposed protocol ensures finite-time convergence of the agent swarm on the reference path

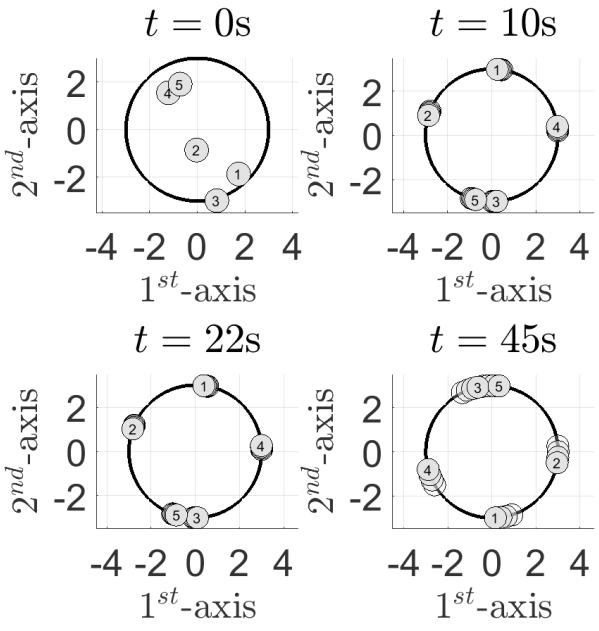

Fig. 4. Example 2: Reference shape $\gamma(\omega)$, in black, and four snapshots of agents' configuration. At $t = 10s,\ 22s,\ 45s$ the direction of motion of the agents is represented by change of transparency (from more transparent to less transparent over time).

while achieving bounded error for each agent evolution with respect to a given reference movement profile.

REFERENCES

Banyaga, A. (2013). *The structure of classical diffeomorphism groups*, volume 400. Springer Science & Business Media.

Chipade, V.S. and Panagou, D. (2021). Multiagent planning and control for swarm herding in 2-d obstacle environments under bounded inputs. *IEEE Transactions on Robotics*, 37(6), 1956–1972. doi: 10.1109/TRO.2021.3072026.

D'Alfonso, L., Franzè, G., and Fedele, G. (2018). Distributed model predictive control for constrained multiagent systems: a swarm aggregation approach. In *2018 Annual American control conference (ACC)*, 5082–5087. IEEE.

Dong, X., Zhou, Y., Ren, Z., and Zhong, Y. (2016). Time-varying formation tracking for second-order multi-agent systems subjected to switching topologies with application to quadrotor formation flying. *IEEE Transactions on Industrial Electronics*, 64(6), 5014–5024.

Dunbabin, M. and Marques, L. (2012). Robots for environmental monitoring: Significant advancements and applications. *IEEE Robotics & Automation Magazine*, 19(1), 24–39.

Egerstedt, M. and Hu, X. (2001). Formation constrained multi-agent control. *IEEE Transactions on Robotics and Automation*, 17(6), 947–951.

Fedele, G. and D'Alfonso, L. (2019). A coordinates mixing matrix-based model for swarm formation. *International Journal of Control*, 1–11.

Fedele, G. and D'Alfonso, L. (2018). A kinematic model for swarm finite-time trajectory tracking. *IEEE Transactions on Cybernetics*, 49(10), 3806–3815.

Fedele, G., D'Alfonso, L., and D'Aquila, G. (2018). Magnetometer bias finite-time estimation using gyroscope data. *IEEE Transactions on Aerospace and Electronic Systems*, 54(6), 2926–2936.

Fedele, G., D'Alfonso, L., and Gazi, V. (2022). A generalized gazi–passino model with coordinate-coupling matrices for swarm formation with rotation behavior. *IEEE Transactions on Control of Network Systems*, 9(3), 1227–1237. doi:10.1109/TCNS.2022.3141012.

Gao, F., Hu, X., Li, S.E., Li, K., and Sun, Q. (2018). Distributed adaptive sliding mode control of vehicular platoon with uncertain interaction topology. *IEEE Transactions on Industrial Electronics*, 65(8), 6352–6361.

Gazi, V. and Passino, K.M. (2011). *Swarm stability and optimization*. Springer Science & Business Media.

Hu, J., Bhowmick, P., Jang, I., Arvin, F., and Lanzon, A. (2021a). A decentralized cluster formation containment framework for multirobot systems. *IEEE Transactions on Robotics*, 37(6), 1936–1955.

Hu, J., Bhowmick, P., and Lanzon, A. (2021b). Group coordinated control of networked mobile robots with applications to object transportation. *IEEE Transactions on Vehicular Technology*, 70(8), 8269–8274.

Khalil, H.K. (2002). Nonlinear systems, 3rd. *New Jewsey, Prentice Hall*, 9(4.2).

Li, S.E., Qin, X., Li, K., Wang, J., and Xie, B. (2017). Robustness analysis and controller synthesis of homogeneous vehicular platoons with bounded parameter uncertainty. *IEEE/ASME Transactions on Mechatronics*, 22(2), 1014–1025.

Liang, K.Y., Mårtensson, J., and Johansson, K.H. (2015). Heavy-duty vehicle platoon formation for fuel efficiency. *IEEE Transactions on Intelligent Transportation Systems*, 17(4), 1051–1061.

Mesbahi, M. and Egerstedt, M. (2010). Graph theoretic methods in multiagent networks. In *Graph Theoretic Methods in Multiagent Networks*. Princeton University Press.

Mwaffo, V., DeLellis, P., and Humbert, J.S. (2021). Formation control of stochastic multivehicle systems. *IEEE Transactions on Control Systems Technology*, 29(6), 2505–2516. doi:10.1109/TCST.2020.3047422.

Reynolds, C.W. (1987). Flocks, herds and schools: A distributed behavioral model. In *Proceedings of the 14th annual conference on Computer graphics and interactive techniques*, 25–34.

Schranz, M., Umlauft, M., Sende, M., and Elmenreich, W. (2020). Swarm robotic behaviors and current applications. *Frontiers in Robotics and AI*, 7, 36.

Warburton, K. and Lazarus, J. (1991). Tendency-distance models of social cohesion in animal groups. *Journal of Theoretical Biology*, 150(4), 473–488.

Xu, L., Zhuang, W., Yin, G., Bian, C., and Wu, H. (2019). Modeling and robust control of heterogeneous vehicle platoons on curved roads subject to disturbances and delays. *IEEE Transactions on Vehicular Technology*, 68(12), 11551–11564.

Zheng, Y., Li, S.E., Wang, J., Cao, D., and Li, K. (2015). Stability and scalability of homogeneous vehicular platoon: Study on the influence of information flow topologies. *IEEE Transactions on Intelligent Transportation Systems*, 17(1), 14–26.